Novel Design Solution to High Precision 3 Axes Translational Parallel Mechanism

T A Dwarakanath and Gaurav Bhutani

Abstract

In this paper, we revisit the 3-Degrees of freedom (DOF) pure translational mechanism. The mathematical model and the design considerations are discussed. A detailed sensitivity analysis is carried out and the results are discussed in a new perspective. The theoretical model makes a strong case for feasibility of simple and practical 3-DOF pure translational mechanism. We validate the theoretical observations with prototype models and experiments. The results concur with the theoretical observations in contrast to what is presented in [6].

Keywords: 3 DOF Spatial Parallel Mechanism, Sensitivity Analysis, Prototype development.

1 Introduction

Spatial 3-DOF pure translational mechanisms are most employed in the industry. Most of them are serial based mechanisms and widely applied in 3-axis cranes, machining centers, Co-ordinate Measuring Machines, etc. Only recently, 3-axis parallel mechanisms are making their entry in the industry through Delta robots in high speed pick and place applications. The nature of fully parallel mechanisms is that they exhibit high stiffness in most of the mechanism workspace [1]. There are robust and interesting theoretical analyses [1-5] presented on the topic. These theoretical works made a strong case for feasibility of simple and practical three degrees of freedom, fully parallel mechanisms. The 3-DOF Spatial Parallel Kinematic Manipulator (SPKM) is the most generalized 3-RRPRR mechanism, wherein in the first and last, two individual revolute joints are replaced with compound universal joints respectively. There are very few research reports based on experimental results. The observations and negative results presented in [6], a general article reviewing the performance indices on parallel manipulators [8] and a kinematic analysis on accuracy of parallel manipulators [9] acknowledging [6] largely shifted the focus away from the mechanism. This shift in focus resulted despite sound theoretical assertions [1-5, 7 and 10-13]. Going by the conflicting results between the theory and the observations based on the practical model, we chose to revisit the mechanism and build a theoretical model, sensitivity analysis and validate it with prototype models and experiments.

T A Dwarakanath (Corresponding Author)
Division of Remote Handling and Robotics, Bhabha Atomic Research Centre, Mumbai 400085, Email: tad@barc.gov.in

Gaurav Bhutani
Division of Remote Handling and Robotics, Bhabha Atomic Research Centre, Mumbai 400085, Email: bhutani@barc.gov.in

2 Kinematic Model and Design Consideration

Simple kinematic analysis suggests that the mechanism based on parallel architecture can possess high accuracy and repeatability. This is because, the end effector motion is generated by actuated links directly connected to the base. The simple kinematic analysis does not reveal the design challenges because of high number of passive joints present in the mechanism. Therefore the influence of passive joint selection or design has to be critically considered in a manipulator design. It is shown in [2] that the 3-RRPRR, 3-DOF SPKM under some geometric conditions results in pure translational motion. Each of the three legs of the manipulator connected to the base through two revolute joints and the platform through two revolute joints has to meet the following conditions

$$q_{2i} = q_{3i} \; and \; q_{1i} = q_{4i}, (i = 1,2,3) \tag{1}$$

Where, q_{1i} and q_{2i} are the unit vectors of passive revolute joint axes at the base and similarly q_{3i} and q_{4i} are the unit vectors of passive revolute joint axes at the platform. While the assembly of the base is made, the three legs and the platform should be under the following geometrical conditions.

$$\left| q_{11} \cdot q_{12} \right| = \left| q_{41} \cdot q_{42} \right|, \left| q_{11} \cdot q_{13} \right| = \left| q_{41} \cdot q_{43} \right|, \left| q_{12} \cdot q_{13} \right| = \left| q_{42} \cdot q_{43} \right| \tag{2}$$

where, q_{ji} is the unit vector of the j^{th} joint of the i^{th} connector.

In this section, we present the engineering design considerations to achieve very closely, what is recommended in the theoretical kinematic design. All the geometric conditions given in the set of equations 1 and 2 are relationships among axes of passive joints. Therefore the design steps, which establish and maintain the geometric conditions, are very important. Two universal joints, each of which is built with common cube blocks with a pair of orthogonal hinges located closely together seems to be a straight forward solution but for the torsional backlash. The presence of torsional backlash affects the accuracy of the manipulator. The universal joints are meant to transmit high torque with minimal direction reversals and are not meant for establishing high precision geometric constraints. A small clearance along the radial direction and close hinge supports would ill define an axis. We have further studied this aspect by constructing a 3-UU system based on single block universal joints. The platform motions are measured and it is found to be less than what is maximum predicted using theoretical models. No disproportionate motion of the platform is observed as indicated in [6]. It is clear from the observations and the readings of the prototype model that the imprecision is due to play at the joints. When we externally arrested the play partially on the joints on one of the connectors, the stiffness of the platform improved significantly. The observation made in 3-UU suggests that a high precision 3-UPU is practical provided that the joint play is eliminated. Instead of closely held pin hinges, distantly separated hinges would considerably reduce the torsional backlash. Also instead of pin and bush, a high precision wide needle bearing will result in near zero torsional backlash. Further reduction in play due to clearance can be arrested by providing an end pre-load by the outside bearing retainers. Such prototypes make a huge difference in stiffness of the platform and trajectory following precision. The prototype development based on this consideration is presented in section 4.

3 Sensitivity Analysis

There can be a point and region around a point in the workspace where the performance can be classified as the best and is the preferred region for the manipulator operations. To identify such regions and in general to understand how the performance indices vary from point to point within a workspace of a manipulator, the sensitivity analysis is carried out. The sensitivity analysis of the manipulator deals with determining the motion of the platform for the given motion of each of its links. For the context, the sensitivity of the platform is defined as the ratio of the rate of change of leg lengths to the rate of change of motion of the platform. This is somewhat different to the pre-assumption that the sensitivity is defined as ratio of the output to the input. Isotropy in sensitivity is a most sought after quality but the sensitivity is not isotropic at all points in the workspace. It is important to determine how the sensitivity would vary in a space to design the workspace for a given range of inputs. The sensitivity at a point also indicates how the leg errors influence the end-effector platform position. The sensitivity is a function of proportion of the manipulator parameters. The size of the base, the size of the platform and the height of the manipulator constitutes the parameter set. The sensitivity indices are obtained as a function of manipulator parameters and the best sensitivity indices for a set of points (workspace) is arrived. In this section, the mathematical model is developed for the sensitivity analysis of a 3-DOF SPKM. A numerical example considering the realistic values for the manipulator parameters is given. In the later section, we also give the details of the prototype development based on the numerical values given in the example and the experimental results are discussed. The figures 1 and 2 show the kinematic sketch and describe the manipulator parameters. The three base connection points are chosen to form an equilateral triangle and so are the connection points at the platform. The co-ordinates of all the points are defined with respect to a global coordinate system fixed at the centre of the base **O** (XYZ) as shown in figures 1 and 2. The above straight forward choice is based on the symmetry. The plane formed by the connection points at the platform is parallel to the base. The height of the manipulator is described as the normal distance from the base to the platform and '*h*' is the initial height of the platform. Let '***b'*** be the side of the base equilateral triangle, and '*a*' be the side of the platform equilateral triangle. l_1, l_2, l_3 are the leg lengths connecting base connector point B_i to the corresponding platform point A_i, i=1, 2, 3. $\hat{i}, \hat{j}, \hat{k}$ are the unit vectors along the **X, Y** and **Z** axes. For the initial or home position of the platform, the coordinates of the centre of platform are given as $[0,0,h]^T$. *(x, y, z)* are the coordinates of the centre of the platform from its initial position. The coordinates of the leg connection points at the base and the platform with respect to **O** (XYZ) are given by

$$B_1 = \left[b/\sqrt{3},0,0\right]^T \qquad B_2 = \left[-b/2\sqrt{3}, b/2, 0\right]^T \qquad B_3 = \left[-b/2\sqrt{3}, -b/2, 0\right]^T$$

$$A_1 = \left[a/\sqrt{3}+x, y, z+h\right]^T \quad A_2 = \left[-a/2\sqrt{3}+x, a/2+y, z+h\right]^T$$

$$A_3 = \left[-a/2\sqrt{3}+x, -a/2+y, z+h\right]^T$$

The three leg vectors from the base connection points to the platform connection points are

$$\vec{l}_1 = \vec{A}_1 - \vec{B}_1; \qquad \vec{l}_2 = \vec{A}_2 - \vec{B}_2 \; ; \qquad \vec{l}_3 = \vec{A}_3 - \vec{B}_3 \tag{3}$$

The inverse kinematics solution is given as

$$\left(a/\sqrt{3} - b/\sqrt{3} + x\right)^2 + y^2 + (z+h)^2 = l_1^{\,2} \tag{4}$$

$$\left(b/2\sqrt{3} - a/2\sqrt{3} + x\right)^2 + (a/2 - b/2 + y)^2 + (z+h)^2 = l_2^{\,2} \tag{5}$$

$$\left(b/2\sqrt{3} - a/2\sqrt{3} + x\right)^2 + (b/2 - a/2 + y)^2 + (z+h)^2 = l_3^{\,2} \tag{6}$$

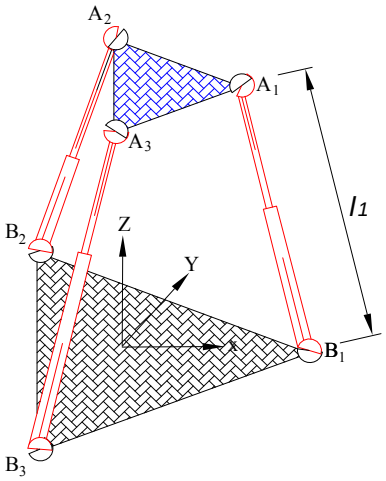

Figure 1: Three DOF SPKM

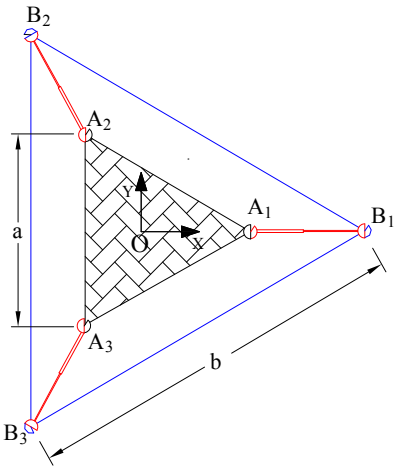

Figure 2: Top view of SPKM to describe kinematic parameters

The sensitivity index of a leg is defined as the rate of change of the leg length with respect to the rate of change of platform position. The sensitivity indices can be determined by differentiating the above inverse kinematic equations. The relation in the matrix form is given as

$$\begin{bmatrix} dl_1 \\ dl_2 \\ dl_3 \end{bmatrix} = \begin{bmatrix} \frac{1}{l_1}\left(a/\sqrt{3} - b/\sqrt{3} + x\right) & \frac{1}{l_1}y & \frac{1}{l_1}(z+h) \\ \frac{1}{l_2}\left(b/2\sqrt{3} - a/2\sqrt{3} + x\right) & \frac{1}{l_2}(a/2 - b/2 + y) & \frac{1}{l_2}(z+h) \\ \frac{1}{l_3}\left(b/2\sqrt{3} - a/2\sqrt{3} + x\right) & \frac{1}{l_3}(b/2 - a/2 + y) & \frac{1}{l_3}(z+h) \end{bmatrix} \begin{bmatrix} dx \\ dy \\ dz \end{bmatrix} \tag{7}$$

The sensitivity indices are given by the members of the 3×3 matrix. The nine sensitivity indices are: $\frac{dl_1}{dx}, \frac{dl_1}{dy}, \frac{dl_1}{dz}, \frac{dl_2}{dx}, \frac{dl_2}{dy}, \frac{dl_2}{dz}, \frac{dl_3}{dx}, \frac{dl_3}{dy}, \frac{dl_3}{dz}$

3.1 Sensitivity with respect to an arbitrary displacement vector

The sensitivity index of a leg with respect to an arbitrary displacement vector $d\vec{r}$ is computed. The position vector of the platform with respect to **O** (XYZ) is given by

$$\vec{r} = x\hat{i} + y\hat{j} + (z+h)\hat{k} \tag{8}$$

Differentiating the above, the displacement vector of the platform is written as

$$d\vec{r} = dx\hat{i} + dy\hat{j} + dz\hat{k} \tag{9}$$

From the previous subsection, the arbitrary leg vector is of the form

$$\vec{l}_i = (x + c_{1i})\hat{i} + (y + c_{2i})\,\hat{j} + (z + c_{3i})\hat{k} \tag{10}$$

$$l_i^2 = (x + c_{1i})^2 + (y + c_{2i})^2 + (z + c_{3i})^2 \tag{11}$$

where c_{1i}, c_{2i}, c_{3i} are constants for a manipulator. Differentiating,

$$l_i dl_i = (x + c_{1i})dx + (y + c_{2i})dy + (z + c_{3i})dz = \vec{l}_i \cdot d\vec{r} \tag{12}$$

The sensitivity index is given by

$$\frac{dl_i}{dr} = \frac{\vec{l}_i \cdot d\vec{r}}{l_i dr} = \hat{l}_i . d\hat{r} = \cos\theta \tag{13}$$

where $\hat{l}_i$ is a unit vector along $\vec{l}_i$, $d\hat{r}$ is a unit vector along $d\vec{r}$, and θ the angle between $\vec{l}_i$ and $d\vec{r}$. The sensitivity index is given by the dot product of the unit leg vector and the unit displacement vector. The dot product is equal to cosine of the angle between the two vectors. For illustration, dl_1 / dx is given by the cosine of the angle between $\vec{l}_1$ and X axis. For the motion of the platform along X axis, the absolute value of the cosine of the angle decreases and hence the dl_1 / dx decreases. For the motion of the platform along Z axes, the absolute value of the cosine of the angle decreases and hence dl_1 / dx decreases. The expression also implies that the change in the leg length is always less than the resultant distance traversed by the platform of the SPKM. For a good sensitivity, we need a higher value of dl / dr.

3.2 Variation of sensitivity indices in manipulator workspace

A SPKM having kinematic parameters, *b = 329 mm; a = 78 mm; h = 132 mm* are considered to characterize sensitivity at various points in the workspace. Translations $-50.0 \le x \le +50.0$; y=0.0; $-50.0 \le z \le +50.0$ are considered for the analysis and the sensitivity at various points inside the workspace are computed. Figures 3, 4 and 5 show the variation of nine sensitivity indices, when the SPKM translates along X axis keeping (*y, z*) coordinates constant at (0,-50), (0, 0) and (0, 50) respectively. Some of the indices show a downward trend and some an upward trend as the values of translation along X and Z axes change. This can be attributed to the variation in angle between the leg vector and the translation vector as discussed earlier. At *z=0, x = 40 mm*, many sensitivity indices tend to approach a closer and higher value. This would be the best isotropic point for the given workspace. The point and the region around it can be chosen as a preferential region in the workspace for the manipulator operation. The position of workspace best suited for a particular translation vector can hence be calculated.

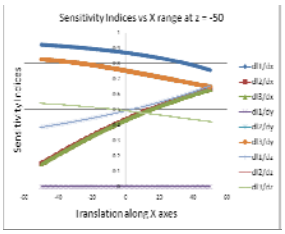

Figure 3: Variation of sensitivity indices along *X* at y=0 and z=-50

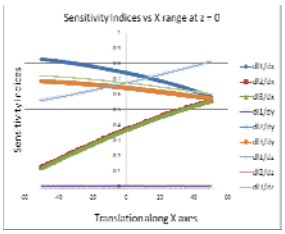

Figure 4: Variation of sensitivity indices along *X* at y=0 and z=0

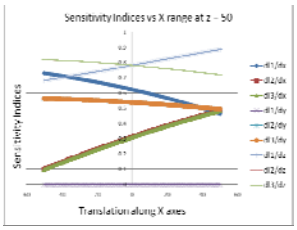

Figure 5: Variation of sensitivity indices along *X* at y=0 and z=50

3.3 Isotropic Sensitivity for three legs

The isotropic sensitivity of the three legs for a given displacement vector at a point in the workspace is important. In other words, it is important to find a translation vector from a point in the workspace, wherein the sensitivities of all the three legs are equal. $\hat{l}_1, \hat{l}_2, \hat{l}_3$ are the unit vectors along the three legs and $d\hat{r}$ is the unit translation vector. The *Isotropic* Sensitivity equation can be written as $\hat{l}_1.d\hat{r} = \hat{l}_2.d\hat{r} = \hat{l}_3.d\hat{r}$**.**From equation 8, 9 and 10, the expression for $\hat{l}_i.d\hat{r}$ is obtained and equating the expressions we get,

$$\frac{1}{l_1}\left[\left(a/\sqrt{3} - b/\sqrt{3} + x\right)dx + ydy + (z+h)dz\right]$$

$$= \frac{1}{l_2}\left[\left(b/2\sqrt{3} - a/2\sqrt{3} + x\right)dx + (a/2 - b/2 + y)dy + (z+h)dz\right]$$

$$= \frac{1}{l_3}\left[\left(b/2\sqrt{3} - a/2\sqrt{3} + x\right)dx + (b/2 - a/2 + y)dy + (z+h)dz\right]$$

The above equation can be solved in two ways. In the first case, the position of the centre of the platform with respect to **O** (XYZ) is taken to be known. That is, $\vec{r} = x\hat{i} + y\hat{j} + (z+h)\hat{k}$ is known, and we calculate the unit displacement vector $\frac{d\vec{r}}{r} = \frac{dx\hat{i} + dy\hat{j} + dz\hat{k}}{r}$. The equations formed would be a set of linear equations giving a single solution. In the second case, we take the unit displacement vector to be given, $\frac{d\vec{r}}{r} = \frac{dx\hat{i} + dy\hat{j} + dz\hat{k}}{r}$, and we determine the position of the platform, $\vec{r} = x\hat{i} + y\hat{j} + (z+h)\hat{k}$ in the workspace. The equations formed would be a set of non linear equations giving multiple solutions for this problem. The set of equations for the first case are

$$\left[\frac{1}{l_1}\left(\frac{a}{\sqrt{3}} - \frac{b}{\sqrt{3}} + x\right) - \frac{1}{l_2}\left(\frac{b}{2\sqrt{3}} - \frac{a}{2\sqrt{3}} + x\right)\right]\frac{dx}{dz} + \left[\frac{1}{l_1}y - \frac{1}{l_2}\left(\frac{a}{2} - \frac{b}{2} + y\right)\right]\frac{dy}{dz} + \left[\frac{1}{l_1}(z+h) - \frac{1}{l_2}(z+h)\right] = 0$$

$$\left[\frac{1}{l_1}\left(\frac{a}{\sqrt{3}} - \frac{b}{\sqrt{3}} + x\right) - \frac{1}{l_3}\left(\frac{b}{2\sqrt{3}} - \frac{a}{2\sqrt{3}} + x\right)\right]\frac{dx}{dz} + \left[\frac{1}{l_1}y - \frac{1}{l_3}\left(\frac{b}{2} - \frac{a}{2} + y\right)\right]\frac{dy}{dz} + \left[\frac{1}{l_1}(z+h) - \frac{1}{l_3}(z+h)\right] = 0$$

Considering the symmetry at *x = 0, y = 0,* and expressing the leg length in terms of manipulator parameters, we get

$$l_1 = l_2 = l_3 = \sqrt{\left(\frac{a}{\sqrt{3}} - \frac{b}{\sqrt{3}}\right)^2 + (z+h)^2}$$

Substituting the above values and solving the equations we get $\frac{dx}{dz} = \frac{dy}{dz} = 0$,

$$\frac{d\vec{r}}{r} = \frac{0\hat{i} + 0\hat{j} + dz\hat{k}}{dz} = \hat{k}$$

It means that for any translation along Z axes (at *x = 0, y = 0)*, the sensitivity of the three legs is equal.

4 Simulation, Prototype Development & Experiments

Based on the design solution, a 3-DOF spatial parallel mechanism is developed. The design and selection of the various components of the required spatial manipulator is done. Prior to the prototype development, workspace analysis and 3D motion simulation of the SPKM is done. The objective of the simulation is to show its interference free mobility and trajectory planning throughout its motion. A software module is developed which takes the desired translations as input; the OpenGL software model shows the sequence of all the translations. The software module is tested for the various trajectories in the workspace. Based on the manipulator parameters and selection of the prismatic joints, the translation workspace of the manipulator is determined. Figure 6 shows the software simulation snapshot and workspace of the manipulator. Figure 7 shows distribution of leg sensitivity, $dl_1/dx, dl_1/dy, dl_1/dz$ on workspace envelopes. The magnitude of leg sensitivity at a point and its distribution in the manipulator workspace not only give good insight in planning the high resolution task space trajectories but also give a good handle to plan the task space activities.

Experiments are conducted to measure the repeatability and trajectory following accuracy for various payloads. Figure 8 shows the prototype of the 3-DOF spatial parallel manipulator performing a high precision job of inserting a 0.8 mm thick needle in a 1 mm hole. Experimental analysis shows the accuracy of the manipulator to be within 30 microns. Detailed discussions of the experimental results are not in the scope of the paper.

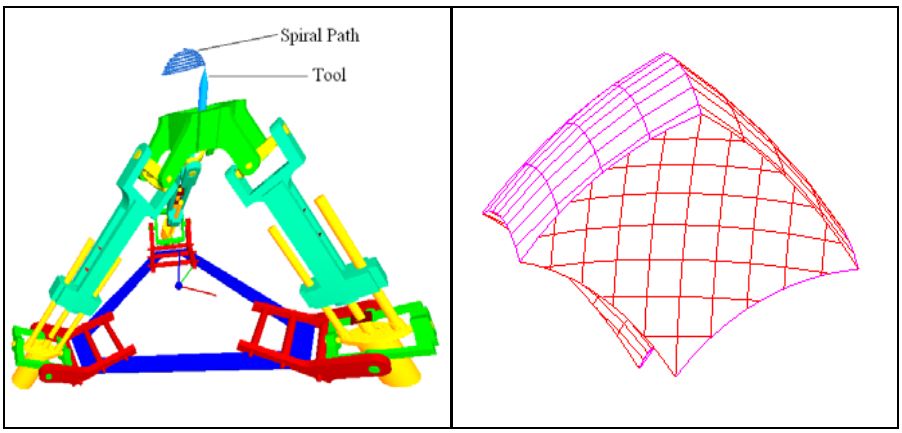

Figure 6: 3D motion simulation and workspace of Spatial Manipulator

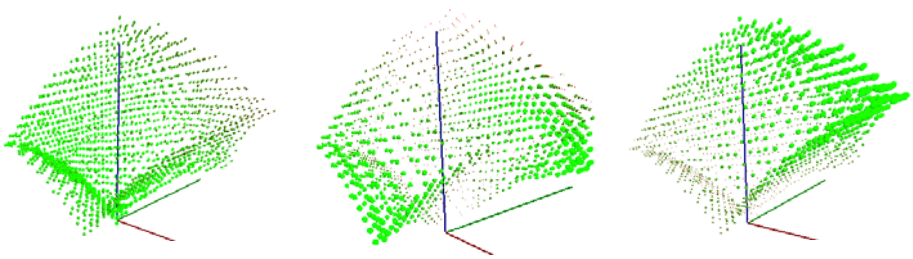

Figure 7: Leg sensitivity distribution, $dl_1/dx, dl_1/dy, dl_1/dz$ on workspace envelope due to positional change along X,Y and Z axes respectively

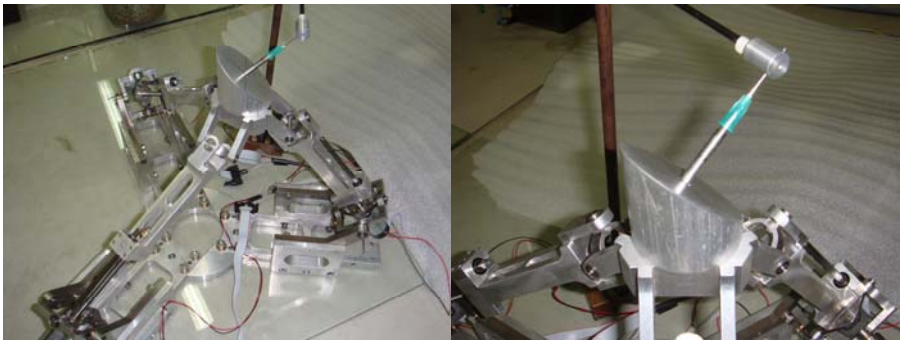

Figure 8: Spatial parallel manipulator performing a high precision job

5 Conclusion

In this paper new design considerations for the development of high accuracy 3-DOF SPKM is discussed. A detailed account of sensitivity analysis is presented. The results obtained from sensitivity analysis greatly help in the synthesis of leg ranges. Based on the design and sensitivity analysis, a prototype 3 DOF SPKM is developed and it is shown that the manipulator exhibit high accuracy and precision. The results are based on the prototype development and the results are in contrast to the results presented in [6] for the similar 3 axis translational parallel manipulator.

References

[1] L. W. Tsai, S. Joshi, ``Kinematics and Optimization of a Spatial 3-UPU Parallel Manipulator,'' Journal of Mechanical Design**,** vol. 122, pp 439-446, 2000.

[2] S. Joshi, L. W. Tsai, ``Jacobian Analysis of Limited-DOF Parallel Manipulators,'' Journal of Mechanical Design, vol. 124, pp. 254-258, 2002.

[3] B. Hu and Y. Lu, ``Solving stiffness and deformation of a 3-UPU parallel manipulator with one translation and two rotations,'' Robotica, published on-line, pp. 1-8, 2011.

[4] D. Gregori, V. P. Castelli, "A Translational 3-DOF Parallel Manipulator," Advances in Robot Kinematics: Analysis and Control, J. Lenarcic and M. L. Husty, eds., Kluwer Academic, pp. 49–58, 1998.

[5] R. D. Gregorio, V. P. Castelli**,** ``Mobility Analysis of the 3-UPU Parallel Mechanism Assembled for a Pure Translational Motion,'' Journal of Mechanical Design, vol. 124(2), pp. 259-264.

[6] C. Han, J. Kim, J. Kim, F. C. Park, ``Kinematic sensitivity analysis of the 3-UPU parallel mechanism,'' Mechanism and Machine Theory, vol. 37, pp. 787–798, 2002.

[7] I. A. Boney, D. Zlatanov, ``The Mystery of the Singular SNU Translational Parallel Robot,'' www.parallemic.org/Reviews/ Review004.html.

[8] J. P. Merlet, ``Jacobian, Manipulability, Condition Number, and Accuracy of Parallel Robots,'' Journal of Mechanical Design, vol. 128(1), pp. 199-206.

[9] J. Meng, D. Zhang, Z. Li, ``Accuracy Analysis of Parallel Manipulators with Joint Clearance,'' Journal of Mechanical Design, vol. 131(1), pp. 1-9.

[10] R. D. Gregorio, "Statics and Singularity Loci of the 3-UPU Wrist," IEEE Transactions on Robotics, vol. 20(4), pp. 630-635, 2004.

[11] S. Joshi, L. W. Tsai, "A Comparison Study of two 3 DOF Parallel Manipulators: One with three and another with four supporting legs," IEEE Transactions on Robotics and Automation, vol. 19(2), pp. 200-209, 2003.
[12] S. Briot, I. A. Bonev, "Accuracy analysis of 3-DOF planar parallel robots," Mechanism and Machine Theory, vol. 43, pp. 445-458, 2008.
[13] Y. Li, Q. Xu, "Kinematic Analysis and Design of a new 3-DOF Translational Parallel Manipulator," Journal of Mechanical Design, vol. 128, pp 729-737, 2006.